

## **IN VITRO BIOCOMPATIBILITY INVESTIGATION OF SILVER AND ZINC MODIFIED HYDROXYAPATITE DEPOSITED ON IMPLANT MATERIALS**

Thi Thanh TRAN<sup>1</sup>, Norica Beatrice NICHITA<sup>2</sup>, Mihaela-Olivia DOBRICA<sup>3</sup>, Cosmin Mihai COTRUT<sup>4</sup>, Maria Diana VRANCEANU<sup>5</sup>, Mihai TARCOLEA<sup>6</sup>

*The purpose of this in vitro study was to evaluate the biocompatibility and bioactivity of silver and zinc modified hydroxyapatite coatings deposited on titanium by electrochemical deposition technique. Preliminary cell culture investigations showed that Ag-HAp and Zn-HAp coating were non-cytotoxic and biocompatible.*

**Keywords:** Biomaterials, hydroxyapatite, biocompatibility, electrochemical deposition

### **1. Introduction**

Titanium (Ti) and its alloys are the most commonly used metallic materials for medical implants in orthopedic and dental applications, due to their low density, non-toxicity, excellent corrosion resistance [1], great biocompatibility and mechanical properties for load bearing orthopedic applications [2]. Even though Ti and its alloys can fulfill most of the clinical requirements which are mandatory in order to properly function in the human body, it is worth mentioning that it also presents some drawbacks. Due to its high affinity for oxygen, Ti is covered with a thin layer of oxide which protects the material from the aggressive media of the human, acting as a barrier. This titanium oxide barrier reduces the osseointegration of titanium and doesn't allow biological interlocking at the bone- titanium implant interface. Thus, to overcome this inconvenient, for many years, surface modification methods for Ti and its alloy have been extensively investigated.

<sup>1</sup> PhD student, Faculty of Materials Science and Engineering, University POLITEHNICA of Bucharest, Romania, e-mail: ttt140483@gmail.com

<sup>2</sup> PhD, Deputy Director of the Institute of Biochemistry of the Romanian Academy, Head of the Viral Glycoproteins Department, norica70@yahoo.co.uk

<sup>3</sup> Researcher, Dept. of Viral Glycoproteins Department, Institute of Biochemistry of the Romanian Academy, mihaelaolivia.dobrica@yahoo.com

<sup>4</sup> Associate Prof., Dept. of Metallic Materials Science, Physical Metallurgy, University POLITEHNICA of Bucharest, Romania, e-mail: cosmin.cotrut@upb.ro

<sup>5</sup> Lecturer, Dept. of Metallic Materials Science, Physical Metallurgy, University POLITEHNICA of Bucharest, Romania, e-mail: diana.vraneanu@upb.ro

<sup>6</sup> Emeritus Prof., Dept. of Metallic Materials Science, Physical Metallurgy, University POLITEHNICA of Bucharest, Romania, e-mail: mihai.tarcolea@upb.ro

In recent years, hydroxyapatite (HAp,  $(\text{Ca}(\text{PO}_4)_6(\text{OH})_2$ ) has been widely used to coat load-bearing metallic implants. The main reason of using HAp coating on metallic substrates is to maintain the mechanical properties of the metal such as load-bearing ability and to use the advantage of the coating which presents a similar chemical composition and biocompatibility with the bone [3]. According to the available literature, several techniques have been used to develop HAp coatings on metallic implants, such as plasma spraying process [4-9], thermal spraying [10], sputter coating [11], pulsed laser ablation [12, 13], dynamic mixing [14], dip coating [15], sol-gel [16, 17], electrophoretic deposition [18], biomimetic coating [19], ion-beam-assisted deposition [20], and hot isostatic pressing [21], electrochemical deposition [22 - 26].

One of the primary features of HAp is the capacity for ion substitution. The ion exchange of HAp with metal ions is promising because it can improve the properties of HAp coating in various applications. Various ions such as  $\text{Cu}^{+2}$  [27, 28],  $\text{Zn}^{+2}$  [27, 29 - 41, 42, 43],  $\text{Ag}^+$  [26, 27, 44 - 74],  $\text{Sn}^{+2}$  [3, 53, 75, 76],  $\text{Mn}^{+2}$  [75],  $\text{Mg}^{+2}$  [75], etc. are incorporated into HAp through substitution  $\text{Ca}^{2+}$  ions. In the present study two metal ions,  $\text{Ag}^+$  and  $\text{Zn}^{2+}$ , respectively, were selected for doping the HAp by electrochemical deposition technique. The samples were investigated by SEM for morphological features and the chemical composition was evidenced by EDS analysis. Moreover, the deposited coatings were evaluated/tested in vitro through biocompatibility and bioactivity assays. In this regard, the in vitro cellular behavior was evaluated on simple and Ag and Zn modified HAp coatings electrochemically deposited on pure titanium. The cell culture used in the resent study consisted in human embryonic kidney 293 cells, HEK 293T cells. Bioactivity behavior of the coatings also were assessed in simulated body fluid (SBF). Several methods have been reported previously to develop simple and modified HAp coatings, including electrochemical deposition [27, 28, 44 - 49, 77 - 81], plasma spray [52 - 58], magnetron sputter coating method [59 - 61], sol-gel synthesis [62 - 65], hydrothermal method [66, 67], wet chemical method [68], the precipitation [69, 70], the dipping [71, 72], the ball milling [73], the ion exchange method [74], etc. To the best of our knowledge there are no studies regarding the addition of Zn into HAp by electrochemical technique, and only through other techniques such as sol-gel process [29, 30], hydrothermal technique [31], ion-exchange [32], precipitation method [33 - 41].

## 2. Materials and Methods

### 2.1 Pretreatments of Ti substrate

The coatings were deposited on commercially pure Ti (cp-Ti, purchased from Bibus Ag Metals, Germany) which acted as substrate. Samples in disc shape with dimension of 14 mm in diameter and 2 mm in thickness were prepared. The substrates were metallographically prepared using different grades of silicon

carbide paper (400 - 800 grit). After, the substrates were thoroughly cleaned with ultrapure water and ultrasonically cleaned in 2-propanol for 20 min and dried in air.

## 2.2 Electrochemical deposition of HAp, Ag-HAp, Zn-HAp coatings on titanium

The electrochemical deposition was carried out with a Potentiostat/Galvanostat Parstat MC, PMC 2000 (Princeton Applied Research, USA) employed to deposit the coatings on Ti, using a typical three cell system configured as following: the Ti substrate was set as working electrode (WE), the platinum foil was the counter electrode (CE) and the saturated calomel electrode (SCE) as reference electrode (RE).

In Table 1 is presented the chemical composition of the electrolytes used in the study. Briefly, the electrolytes were obtained by dissolving the salts (analytical grade, purchased from Sigma Aldrich) in ultra-pure water, ASTM I (Milli-Q). The pH value of electrolyte was adjusted to 5.0 by addition of 1M NaOH. The electrolyte was purged with nitrogen gas for 20 min prior the experiments in order to reduce the hydrogen evolution. During the deposition the electrolytes were continuously stirred. The experiments were performed at 75°C by applying a constant current density of - 0.85 mA/cm<sup>2</sup> for 1200s. After the deposition, the samples were gently rinsed in distilled water and dried in air.

Table 1  
Chemical composition of the electrolyte and samples codification

Substrate	Sample codification	Chemical composition (mM)				(Ca+M)/P (M=Ag, Zn)
		Ca(NO <sub>3</sub> ) <sub>2</sub> ·4H <sub>2</sub> O	NH <sub>4</sub> H <sub>2</sub> PO <sub>4</sub>	Ag(NO <sub>3</sub> )	Zn(NO <sub>3</sub> ) <sub>2</sub> ·6H <sub>2</sub> O	
cp-Ti	HAp	10	6	-	-	1,67
	HAp-Ag	9.975		0.025	-	1,67
	HAp-Zn	9.975		-	0.025	1,67

## 2.3 Characterization and composition analysis of coatings

The morphology and element distribution of the coatings were studied using scanning electron microscopy equipped (SEM) with an energy dispersive spectroscopy (EDS) (Phenom ProX, Phenom World, Netherlands).

## 2.4 In vitro biological activity analysis

Bioactivity was evaluated by soaking the coated specimens in 40 mL of simulated blood fluid solution (SBF). The chemical composition of the media (Table 2) used in the present study resemblance to human blood plasma and uses the receipt proposed by Kokubo [82, 83]. The tests were achieved at 37°C for 21 days and at different periods of 1, 3, 7, 14, 21 days samples were removed from

the media and gently washed with distill water and then dried in a desiccator. The SBF was refreshed every 3 days to preserve the ions concentration.

Table 2

**The chemical composition of SBF media (1000 mL)**

NaCl (g)	NaHCO <sub>3</sub> (g)	KCl (g)	K <sub>2</sub> HPO <sub>4</sub> ·3H <sub>2</sub> O (g)	MgCl <sub>2</sub> ·6H <sub>2</sub> O (g)	1M HCl mL	CaCl <sub>2</sub> (g)	Na <sub>2</sub> SO <sub>4</sub> (g)	Tris (g)
8.035	0.355	0.225	0.231	0.311	3.2	0.292	0.072	6.118

The samples mass (substrate and coating) evolution was gravimetrically monitored using an analytical balance with an accuracy of 0.01 mg. The weight variation of the formed/lost mass on the surface was determined using the following equation:

$$\Delta m = m_f - m_i$$

where  $\Delta m$  represents the mass variation on the surface,  $m_f$  and  $m_i$  are sample weights before and after exposure to SBF media.

## 2.5 Evaluation of biocompatibility

### 2.5.1 Cell culture

Human embryonic kidney 293T cells (HEK293T) were used to assess the biocompatibility of HAp, HAp-Ag, HAp-Zn coatings. HEK293T were cultured in Dulbecco's modified eagle medium 1X (DMEM), supplemented with Glutamax-I (Life technologies), 10% FBS (Life technologies) and 1% Non-essential amino acids (Life technologies).

Cells were seeded on the Ti samples that were placed in 24-well polystyrene cell culture plates (internal well diameter is 15 mm) and previously rinsed twice with ethanol 70%. Cells seeded on 24-well plates served as control.

Cells were seeded onto the samples at an initial density of 25.000 cells/well and were cultured for 1, 3, and 4 days at 37°C under a humidified air atmosphere consisting of 5% CO<sub>2</sub> and 95% air. The cells were seeded and further were used for cell proliferation assay or stained for immunofluorescence. Culture medium was renewed every 2 days.

### 2.5.2 Immunofluorescence assay

#### 2.5.2.1 Sample preparation

After 24 h culture, the extracellular media was removed, the cells were washed with Dulbecco's Phosphate Buffered Saline (DPBS (1X), Life technologies) and fixed with Paraformaldehyde 4% (PFA 4%) for 20 min at room temperature. Further, the cells were washed again with DPBS 1X, followed by permeabilization with detergent Triton X-100 0.2% in PBS for 4 min and washing

with DPBS (1X). Subsequently, blocking was performed using Bovine serum albumine 1% (BSA) in phosphate buffer solution (PBS) 1X.

#### **2.5.2.2 Staining procedure**

##### **a) Staining for Actin and Ki67**

Cells seeded on the Ti samples were stained with Alexa Fluor® 594 phalloidin (A594) 1/40 in BSA 1% for 60 min. Further, the samples were incubated with anti-Ki67 antibody (rabbit, Thermo Scientific) 1/200 in BSA 1% for 30 min and further with anti-rabbit Alexa Fluor 488 secondary antibody, dilution 1/500 in BSA 1%, for 30 min. Cells were washed 5 times with PBS after each incubation. After staining, samples were mounted on glass slides using Anti-fade solution with DAPI (Invitrogen).

##### **b) Staining for Tubulin and PDI**

Cells seeded on the samples were incubated with Anti-Tubulin antibody (rabbit, Abcam) 1/1000 in BSA 1% for 30 min and further with Anti-Rabbit Alexa Fluor-A594 secondary antibody, 1/500 in BSA 1% for 30 min.

Afterwards, samples were stained with Anti-PDI antibody (mouse, Abcam) 1/1000 in BSA 1% for 30 min, followed by incubation with anti-mouse Alexa Fluor 488 secondary antibody, 1/500 in BSA 1%, for 30 min. Cells were washed 5 times with PBS after each incubation. After staining, samples were mounted on glass slides using Anti-fade solution with DAPI (Invitrogen).

##### **c) Microscopic immunofluorescence analysis**

The cells were visualized under Microscope (ApoTome.2, AXIO) at a magnification 20 X (mode: dry) and 63 X (mode: oil, immersol 518F), respectively.

#### **3.5.3 Cell proliferation assay**

Cells were counted at days 1, 3 and 4 using a hemocytometer. A dilution of the mixture with the number of cells to be counted should be used Trypan Blue Stain 0.4% (T10282, USA) was used to stain the dead cells and calculate cell viability (volumetric ratio 1:1).

The biocompatibility tests were performed in triplicate using different samples to ensure the validity of the results. Means and standard deviations were also calculated.

$$\text{Cell viability (\%)} = \frac{\text{Number of Cell alive}}{\text{Total cell}} \times 100$$

### **3. Results and discussions**

#### **3.1 Morphological investigation**

Fig. 1 shows the scanning electron microscope (SEM) image for simple and modified HAp coatings prepared by the electrochemical deposition method. The images are clearly visible in Fig. 1(a) that the electrodeposited of simple HAp

coating presents a morphology made of ribbon-like crystals and a Ca/P ratio of 1.47.

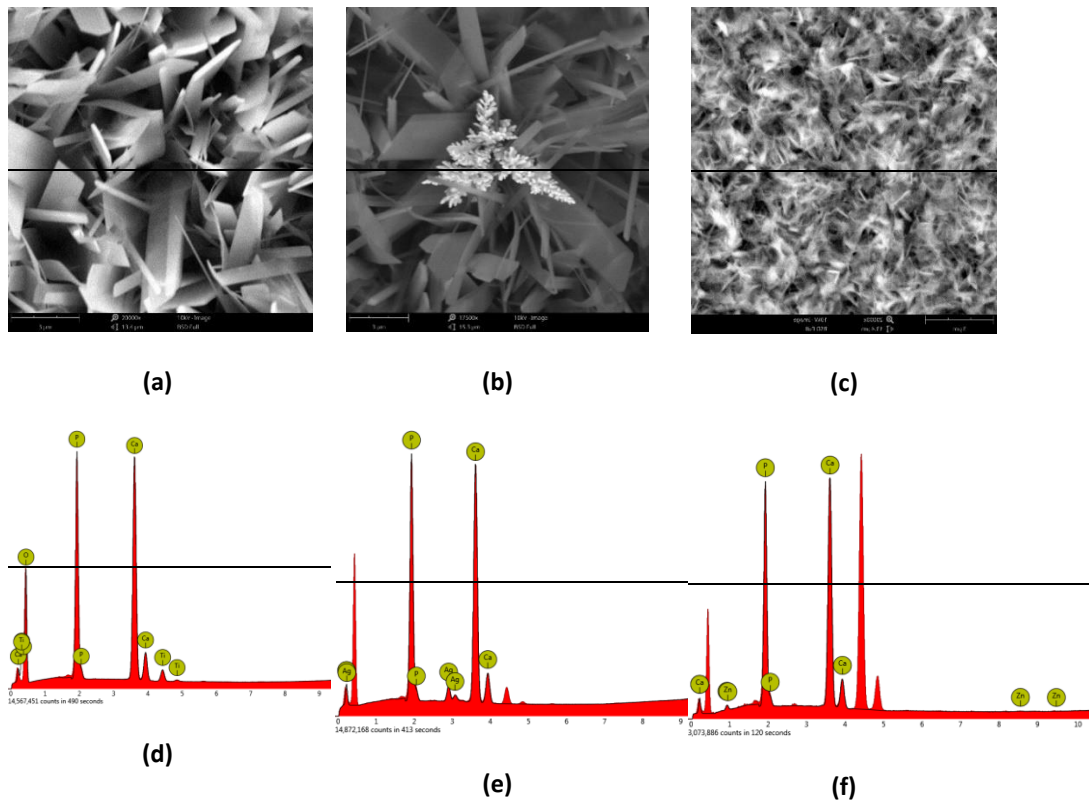


Fig. 1. The SEM/EDS measurements on substrate material:  
HAp (a, d), HAp-Ag (b, e), HAp-Zn coatings (c, f).

The addition of Ag into HAp hasn't modified the plate-like morphology of HAp but some silver particle agglomerations are visible on the HAp crystals Fig. 1(b). In this case the Ca/P ratio is about 1.67 which is similar to the stoichiometric HAp (Ca/P=1.67). The HAp-Zn coatings is characterized by an interconnected network made of very thin and small crystals (Fig. 1.c) suggesting that the morphology of HAp is visible modified by addition of zinc. The Ca/P ratio registered a value of 1.62 which is very close to the stoichiometric one.

According to the EDS analysis, it can be noted that all characteristic elements were identified (Ca, P and O) and also the silver and zinc signals appear on the spectra Fig. 1(e, f).

Thus, it can be said that the addition of Ag and Zn has induced some small modifications in the HAp and also the Ca/P ratio has increased from a value of 1.47 in the case of HAp coatings to 1.67 and 1.62 for HAp-Ag and HAp-Zn, respectively.

### 3.2 Evaluation of Bioactivity

Immersion in SBF media has commonly been used to study the bioactivity of materials as a quick, easy and low-cost method. The SBF used was according to the bioactivity evaluation of the implant materials via the formation of apatite layers on surface of substrates (ISO 23317:2014) and is an important feature in order to estimate the material ability to bond with living tissues. After every period of 1, 3, 7, 14, 21 days immersion in SBF, a thick and dense apatite layer was formed on the specimen surface, minerals crystals covered almost the surface of the specimen. The growth of apatite layers was measured carefully and the obtained values are presented in Table 3. Each sample was measured five times.

Table 3  
Mass evolution of the newly apatite layer on substrate after immersion in SBF

Sample	Mass [mg]				
	Day 1	Day 3	Day 7	Day 14	Day 21
cp-Ti	0.01 ( $\pm 0.01$ )	-0.01 ( $\pm 0.01$ )	0.01 ( $\pm 0.01$ )	0.01 ( $\pm 0.01$ )	2.62 ( $\pm 0.01$ )
HAp	0.51 ( $\pm 0.01$ )	0.71 ( $\pm 0.01$ )	1.19 ( $\pm 0.01$ )	2.08 ( $\pm 0.01$ )	4.58 ( $\pm 0.01$ )
HAp-Ag	0.41 ( $\pm 0.01$ )	1.25 ( $\pm 0.01$ )	2.59 ( $\pm 0.01$ )	3.60 ( $\pm 0.01$ )	7.11 ( $\pm 0.01$ )
HAp-Zn	0.17 ( $\pm 0.01$ )	1.11 ( $\pm 0.01$ )	2.48 ( $\pm 0.01$ )	3.41 ( $\pm 0.01$ )	4.38 ( $\pm 0.01$ )

A slight increase in the initial mass was observed on all the samples after one day exposure to SBF media, except Ti substrate without coating which didn't present any mass changes. The apatite growth rate on HAp-Ag is the fastest at each period. For HAp-Zn samples, the growth rate of the new apatite layer was higher compared to HAp samples at 7 days and 14 day but smaller than at 21 days (Fig. 2). Hence, the bioactivity sequence of the coatings was HAp-Ag > HAp-Zn > HAp > Ti. The presence of bone-like apatite layers on the substrate has been considered as a positive biological response to host.

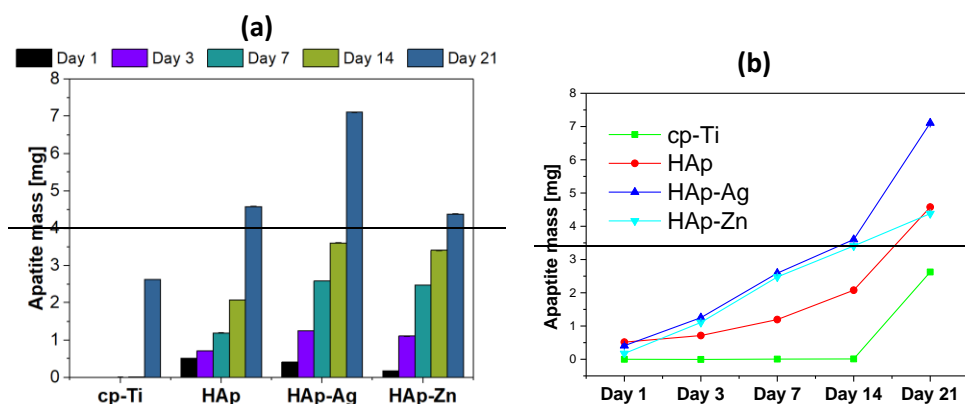
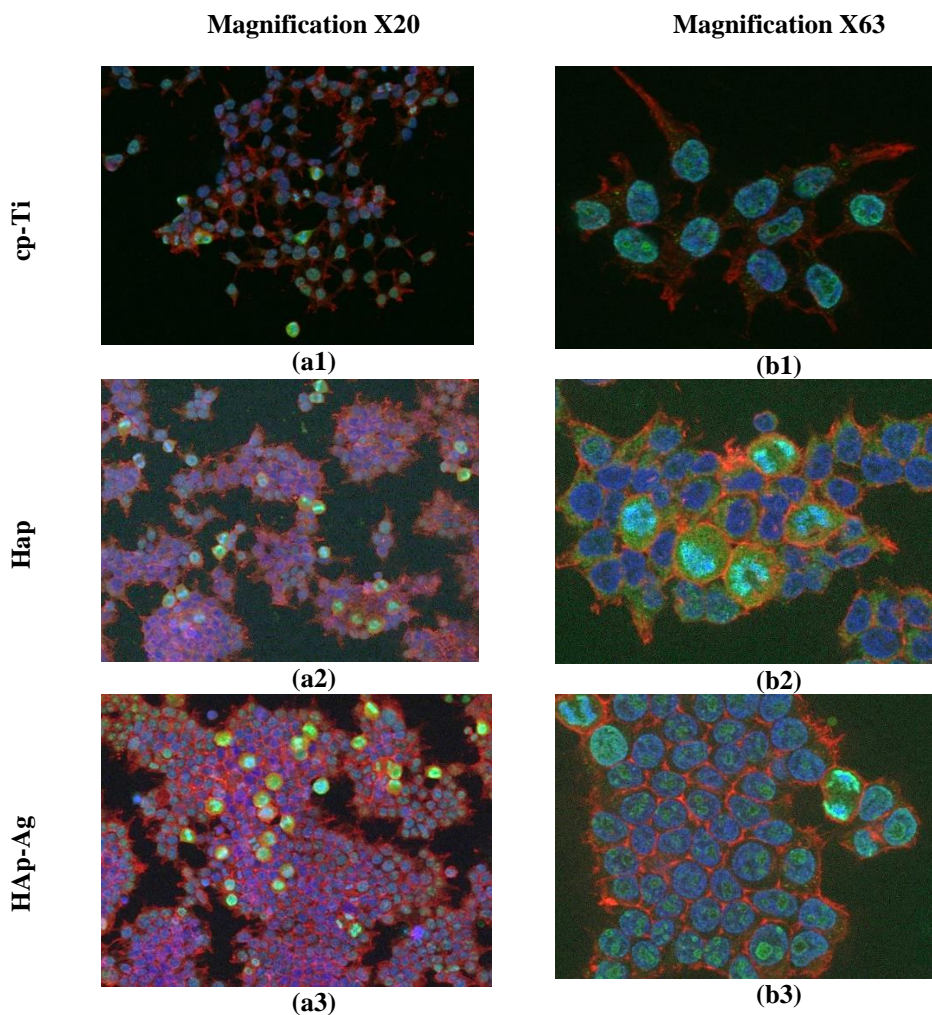


Fig. 2. The chart shows the increase in the mass of the apatite layer on Ti

### 3.3 Evaluation of biocompatibility

#### 3.3.1 Cell morphology

Cell morphology was analyzed by staining the cells for cytoskeletal proteins as actin and tubulin. The actin filaments (polymerized actin) were visualized using phalloidin. No significant differences in the cell's morphology was noted (Fig. 3 and Fig. 4). A reduced polymerization of actin was observed for all the coatings (HAp, HAp-Zn and HAp-Ag) compared to the Ti samples (Fig. 5), suggesting the HAp coatings alter the organization of actin in filaments.



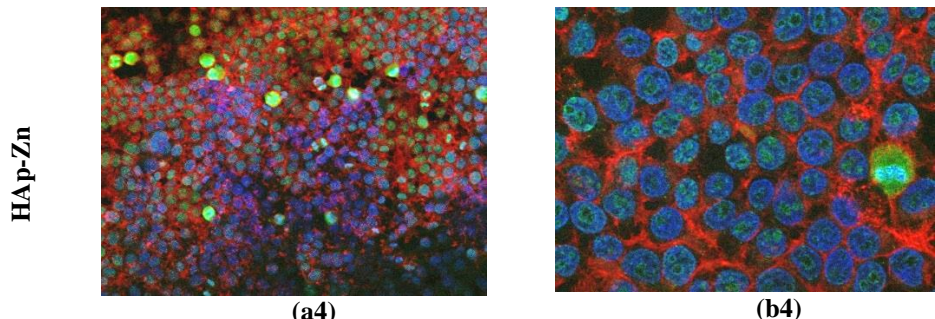
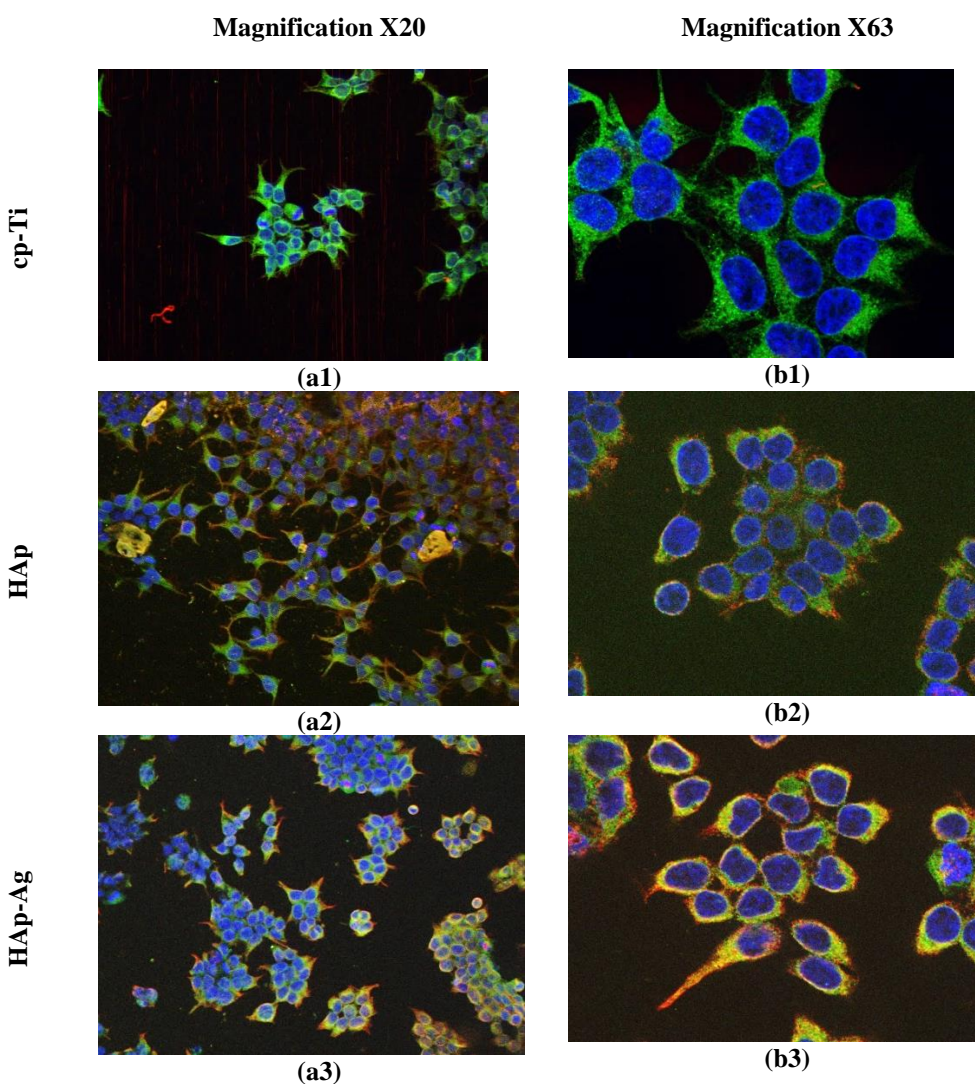


Fig. 3 Fluorescence microscope images of cells stained for actin and Ki67 of the HEK 293T cells (actin-red, Ki67-green)



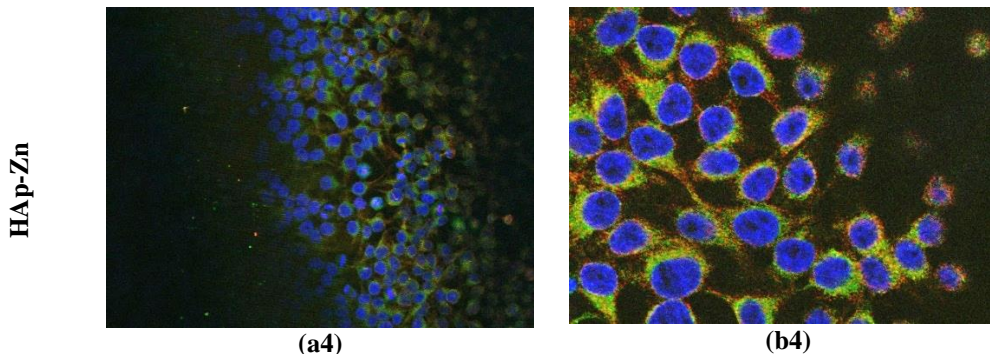
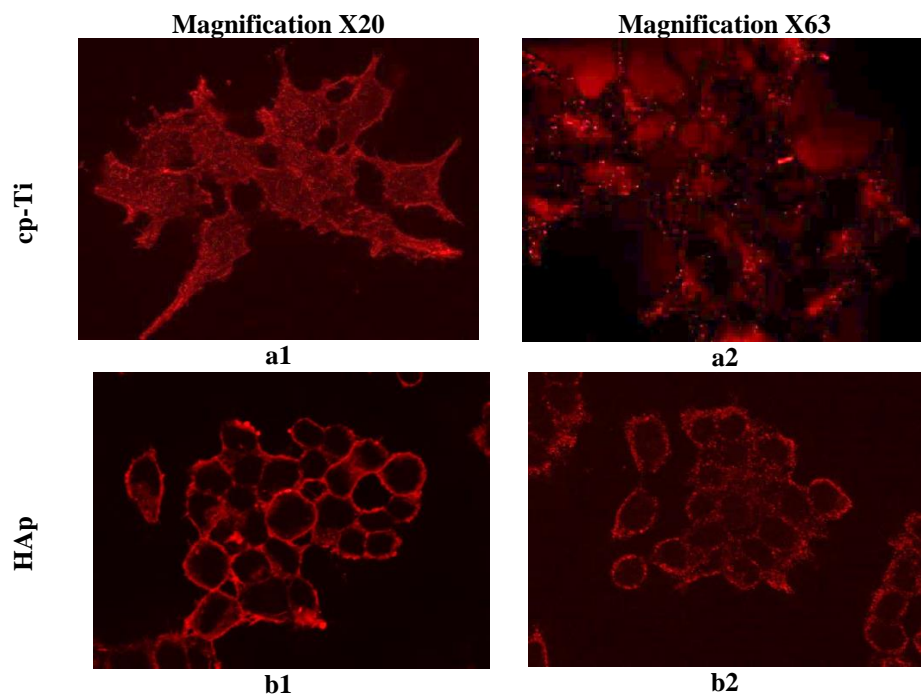


Fig. 4 Fluorescence microscope images of HEK 293T cells stained for tubulin and PDI of the HEK 293T cells (PDI-green, Tubulin-red)

Tubulin staining revealed a better organization of the microtubules in the cells seeded onto HAp-Zn and HAp-Ag than those seeded onto cp-Ti or HAp (Fig.5). This suggest that  $Zn^{2+}$  and  $Ag^+$  ions could add a benefit for tubulin polymerization, which is an important dynamic process for cell intracellular transport and cell division.



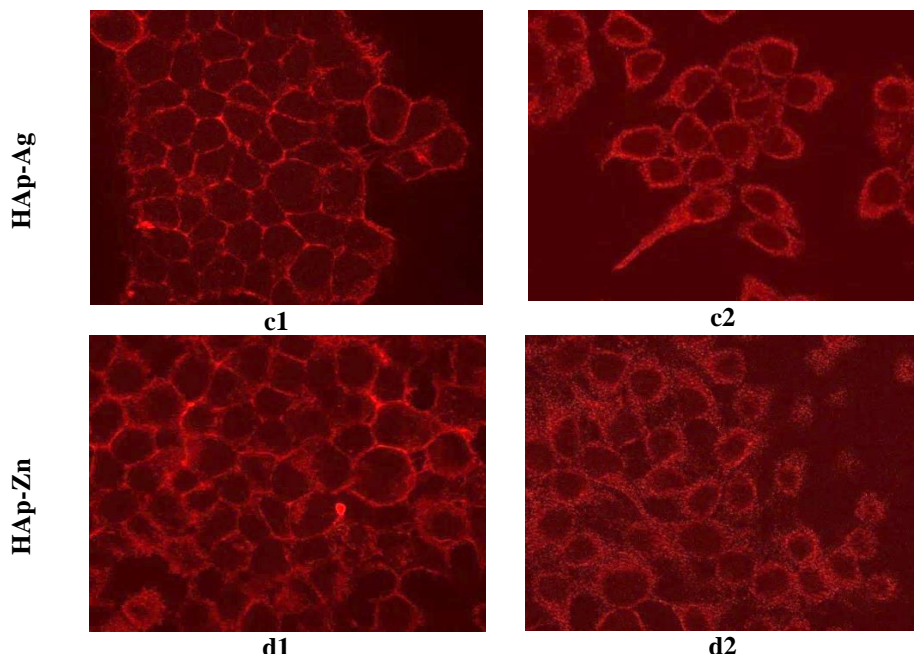


Fig.5. Fluorescence microscope images of HEK 293T cells stained for actin (a1, b1, c1, d1) and tubulin (a2, b2, c2, d2)

The intracellular transport is also related to the function of reticulum endoplasmic, which was evaluated by staining for a specific protein, called protein-disulphide-isomerase (PDI). PDI expression was similar in cells grown on either material (Fig. 6). To evaluate cell proliferation, HEK293T cells were also stained for Ki67 protein, which is associated with this process. It is expressed during G1(growth phase), S (synthesis phase), G2 (gap phase) and mitosis phases of cell cycle, but not in G0 (metabolic state). As it is shown in Fig. 6, Ki67 expression was identified for the majority cells seeded on all samples. A higher level of Ki67 protein was found in cells during mitosis phase, fact confirmed by visualizing the separation of chromosomes during mitosis (prophase, metaphase, telophase and anaphase) by staining with DAPI. Comparison between cell number (by DAPI staining) on the different samples indicates a higher proliferation rate for cells grown on HAp-Zn and HAp-Ag coatings and the lowest on the control sample, cp-Ti.

These results suggest a possible advantage of using HAp-Zn and HAp-Ag coatings to improve cell growing parameters, but further experiments should be carried out using other types of cells.

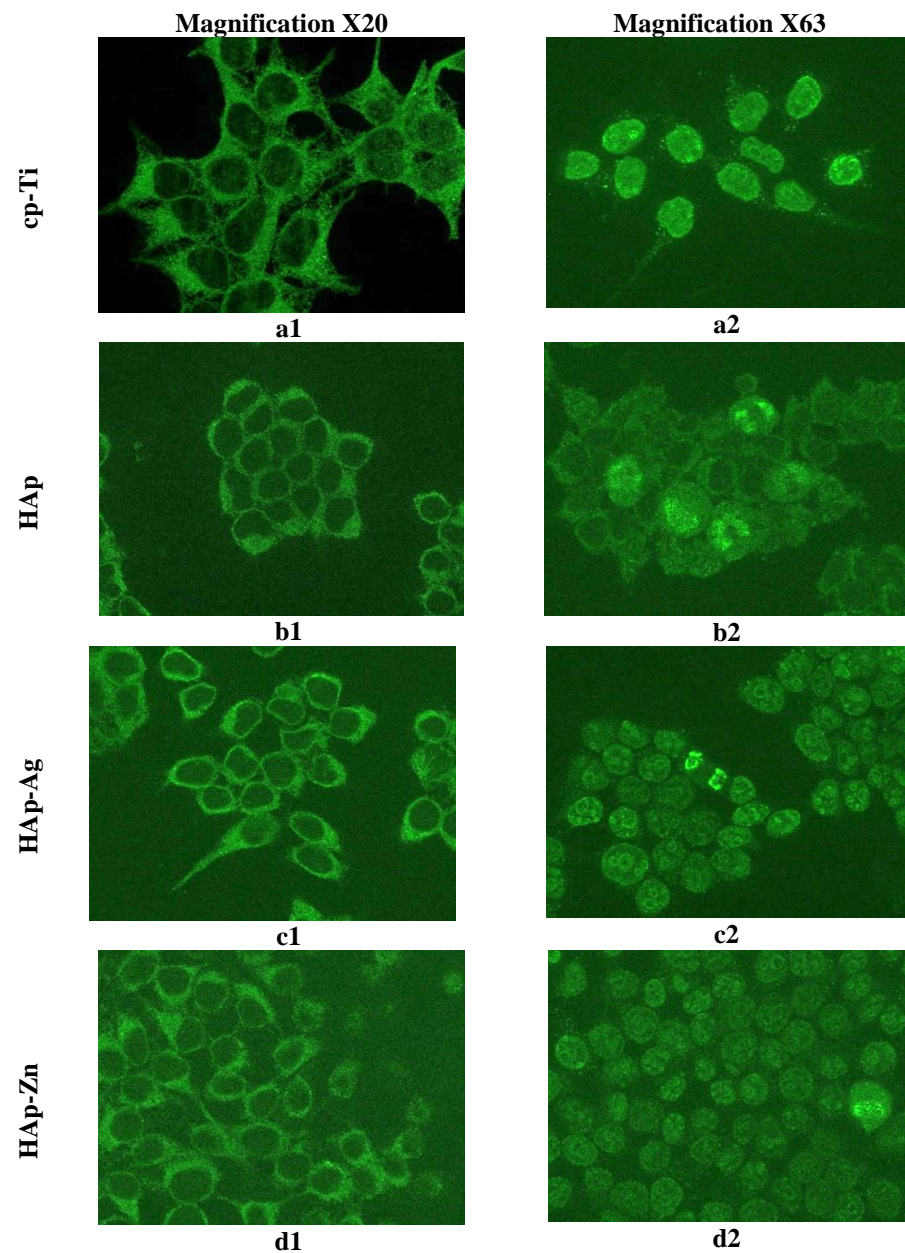


Fig.6. Fluorescence microscope images of HEK 293T cells stained for PDI (a1, b1, c1, d1) and for Ki67 (a2, b2, c2, d2)

### 3.3.2 Cell proliferation

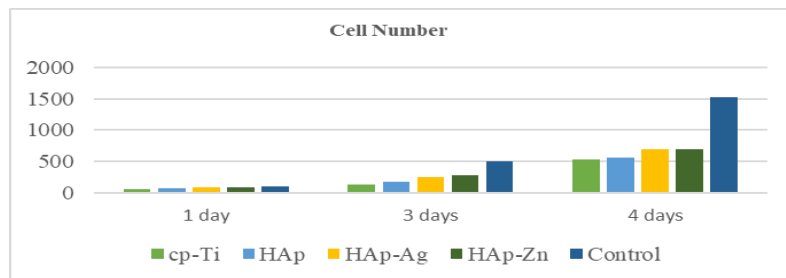


Fig. 7. Cell proliferation on the tested materials after 1, 3 and 4 days.

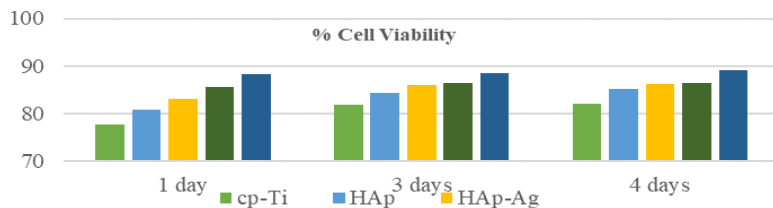


Fig. 8. Cell viability on the tested materials after 1, 3 and 4 days

In Fig. 7 are presented the values obtained for the cell proliferation assay. It can be observed that on day 1 no significant differences were noted between all tested materials. On day 3, a slight increase of cells was observed on all materials. Compared to control sample, the lowest cell proliferation was registered for the uncoated cp-Ti and sequence of the increase rate was cp-Ti < HAp < HAp-Ag < HAp-Zn < control. Similarly, a constantly increase on day 4 was observed on all the samples. Thus, according to cell proliferation assay, it can be said that all coatings have enhanced the cell proliferation on cp-Ti, but better results were noted for HAp coatings with addition of Ag and Zn.

In Fig. 8 are presented the cell viability results which demonstrated that all the samples have good cytocompatibility of HEK 293T cells. *In vitro* biocompatibility clearly indicated that all tested samples showed no cell cytotoxic activity. The cell viability was above 80% (non-cytotoxic), the highest values being obtained for HAp-Zn coatings (86.41 % at day 4). Moreover, on the 4th day, the cell viability was similar for all coatings as following: HAp (85.14 %), HAp-Ag (86.19 %) and HAp-Zn coating (86.41 %). There are no significant differences found between them at day 1 and day 3.

## 4. Conclusions

In the present study, biocompatibility and bioactivity of simple and Ag and Zn modified HAp deposited by electrochemical deposition on pure titanium was evaluated. Based on the presented results the following conclusions were drawn:

- the morphology of HAp was made of thin ribbon-like crystals; the addition of Ag into HAp didn't induce major modification of the ribbon like morphology, but some Ag particle agglomerations were noted; in the case of HAp-Zn coatings, the morphology was made of very thin crystals which formed an interconnected porous network, suggesting that Zn alters the nucleation kinetics;
- the elemental composition indicated that the addition of Ag and Zn enhances the Ca/P ratio of HAp from a value of 1.49 for simple HAp to 1.62 for HAp-Zn and 1.67 for HAp-Ag, the latter ones being close to the stoichiometric HAp (1.67);
- in terms of bioactivity, all coatings have enhanced the biominerization ability of cp-Ti; after 21 days of immersion in SBF the highest values were registered for HAp-Ag coatings (7.11 mg), followed by HAp (4.58 mg) and HAp-Zn (4.38 mg), while the cp-Ti have registered the smallest value (2.11 mg);
- the preliminary cell culture investigations showed that Ag-HAp and Zn-HAp coating were non-cytotoxic and biocompatible and overall addition of Ag and Zn into HAp enhanced the behavior of HAp.

As a conclusion, it can be said that HAp based coatings with small amounts of Ag and Zn can improve the bioactivity and biocompatibility of titanium and can be considered as potential materials for medical application usage.

### Acknowledgements

This work was supported by grants of the Romanian Ministry of Research and Innovation, CCCDI – UEFISCDI, projects number PN-III-P1-1.2-PCCDI-2017-0239/60PCCDI 2018.

### R E F E R E N C E S

- [1] Brunette DM, Titanium in medicine: material science, surface science, engineering, biological responses, and medical applications, Springer Verlag Engineering, Materials; 2001
- [2] M. Long, H.J. Rack, *Biomaterials*, 19 (1998), p. 1621
- [3] Silva P, Santos J, Monteiro F, Knowles J, Adhesion and microstructural characterization of plasma-sprayed hydroxyapatite/glass ceramic coatings onto Ti-6Al-4V substrates, *Surface and Coatings Technology* 1998; 102:191–6.
- [4] De Groot K, Geesink R, Klein C, Serekian P, Plasma sprayed coatings of hydroxyapatite, *Journal of Biomedical Materials Research* 2004;21:1375–81.
- [5] Y.P. Lu, Y. Jiao, J.H. Wang, W.H. Xu, G.Y. Xiao, R.F. Zhu, A further insight into pores in plasma sprayed hydroxyapatite coating, *Surf. Coat. Technol.*, 206 (2012), p. 3550
- [6] L. Sun, C.C. Berndt, K.A. Gross, A. Kucuk, Material fundamentals and clinical performance of plasma-sprayed hydroxyapatite coatings: a review, *J. Biomed. Mater. Res. B Appl. Biomater.*, 58 (2001), p. 570
- [7] V. Sergo, O. Sbaizer, D.R. Clarke, Mechanical and chemical consequences of the residual stresses in plasma sprayed hydroxyapatite coatings, *Biomaterials*, 18 (1997), p. 477

- [8] M. Roy, A. Bandyopadhyay, S. Bose, Induction plasma sprayed nano hydroxyapatite coatings on titanium for orthopaedic and dental implants, *Surf. Coat. Technol.*, 205 (2011), p. 2785
- [9] Y. Yang, K.-H. Kim, J.L. Ong, A review on calcium phosphate coatings produced using a sputtering process—an alternative to plasma spraying, *Biomaterials*, 26 (2005), p. 327
- [10] Gross KA, Berndt CC. Thermal processing of hydroxyapatite for coating production. *Journal of Biomedical Materials Research* 1998; 39:580–7.
- [11] Ding S-J, Properties and immersion behavior of magnetron-sputtered multilayered hydroxyapatite/titanium composite coatings, *Biomaterials* 2003; 24:4233–8.
- [12] Cleries L, Martinez E, Fernandez-Pradas J, Sardin G, Esteve J, Morenza J, Mechanical properties of calcium phosphate coatings deposited by laser ablation, *Biomaterials* 2000;21:967–71.
- [13] K. Van Dijk, H.G. Schaeken, J.G.G. Wolke, J.A. Jansen, Pulsed laser deposition of hydroxyapatite thin films, *Biomaterials*, 17 (1998), p. 159
- [14] Yoshinari M, Ohtsuka Y, Dérand T, Thin hydroxyapatite coating produced by the ion beam dynamic mixing method, *Biomaterials* 1994;15: 529–35.
- [15] Kaciulis S, Mattogno G, Napoli A, Bemporad E, Ferrari F, Montenero A, et al, Surface analysis of biocompatible coatings on titanium, *Journal of Electron Spectroscopy and Related Phenomena* 1998; 95:61–9.
- [16] Li P, Groot Kd, Kokubo T. Bioactive Ca<sub>10</sub>(PO<sub>4</sub>)<sub>6</sub>(OH)<sub>2</sub>/TiO<sub>2</sub> composite coating prepared by sol–gel process. *Journal of Sol–Gel Science and Technology* 1996; 7:27–34.
- [17] P. Choudhury, D.C. Agrawal. Sol–gel derived hydroxyapatite coatings on titanium substrates. *Surf. Coat. Technol.*, 206 (2011), p. 360
- [18] Han Y, Fu T, Lu J, Xu K. Characterization and stability of hydroxyapatite coatings prepared by an electro-deposition and alkaline-treatment process. *Journal of Biomedical Materials Research* 2000; 54 :96–101.
- [19] Habibovic P, Barrere F, Blitterswijk CA, Groot K, Layrolle P. Biomimetic hydroxyapatite coating on metal implants. *Journal of the American Ceramic Society* 2002; 85:517–22.
- [20] Choi J-M, Kim H-E, Lee I-S. Ion-beam-assisted deposition (IBAD) of hydroxyapatite coating layer on Ti-based metal substrate. *Biomaterials* 2000; 21:469–73.
- [21] Wie H, Herø H, Solheim T. Hot isostatic pressing-processed hydroxyapatite coated titanium implants: light microscopic and scanning electron microscopy investigations. *The International Journal of Oral & Maxillofacial Implants* 1998; 13:837.
- [22] M. Manso, C. Jimenez, C. Morant, P. Herrero, J.M. Martinez-Duart. Electrodeposition of hydroxyapatite coatings in basic conditions. *Biomaterials*, 21 (2000), p. 1755
- [23] M.H. Ma, W. Ye, X.X. Wang. Effect of supersaturation on the morphology of hydroxyapatite crystals deposited by electrochemical deposition on titanium. *Mater. Lett.*, 62 (2008), p. 3875
- [24] Y.Y. Zhang, J. Tao, Y.C. Pang, W. Wang, T. Wang. Electrochemical deposition of hydroxyapatite coatings on titanium. *Trans. Nonferrous Metals Soc. China*, 16 (2006), p. 633
- [25] X.J. Zhang, D.Y. Lin, X.H. Yan, X.X. Wang. Evolution of the magnesium incorporated amorphous calcium phosphate to nano-crystallized hydroxyapatite in alkaline solution. *J. Cryst. Growth*, 336 (2011), p. 60
- [26] Y.Y. Yan, X.J. Zhang, Y. Huang, Q.Q. Ding, X.F. Pang. Antibacterial and bioactivity of silver substituted hydroxyapatite/TiO<sub>2</sub> nanotube composite coatings on titanium. *Appl. Surf. Sci.*, 314 (2014), p. 348
- [27] F. Bir, H. Khireddine, A. Touati, D. Sidane, S. Yala, H. Oudadesse, Electrochemical depositions of fluoro-hydroxyapatite doped by Cu<sup>2+</sup>, Zn<sup>2+</sup>, Ag<sup>+</sup> on stainless steel substrates, *Applied Surface Science* 258 (2012) 7021–7030
- [28] Daniela BAJENARU-GEORGESCU, Daniela IONITA, Mariana PRODANA, Ioana DEMETRESCU, Electrochemical and antibacterial characterization of thermally treated titanium biomaterials, *U.P.B. Sci. Bull., Series B*, Vol. 77, Iss. 4, 2015 ISSN 1454-2331
- [29] S.J. Kalita, H.A. Bhatt, Nanocrystalline hydroxyapatite doped with magnesium and zinc: synthesis and characterization, *Mater. Sci. Eng. C* 27 (2007) 837–848.
- [30] R.J. Chung, M.F. Hsieh, C.W. Huang, L.H. Perng, H.W. Wen T.S. Chin, Antimicrobial effects and human gingival biocompatibility of hydroxyapatite sol–gel coatings, *J. Biomed. Mater. Res.* 76B (2006) 169–178.

[31] M. Li, X. Xiao, R. Liu, C. Chen, L. Huang, Structural characterization of zinc-substituted hydroxyapatite prepared by hydrothermal method, *J. Mater. Sci.-Mater. Med* 19 (2008) 797–803

[32] S. Hayakawa, K. Ando, K. Tsuru, A. Osaka, E. Fujii, K. Kawabata, et al., Structural characterization and protein adsorption property of hydroxyapatite particles modified with zinc ions, *J. Am. Ceram. Soc.* 90 (2007) 565–569.

[33] S.C. Cox, P. Jamshidi, L.M. Grover, K.K. Mallick, Preparation and characterization of nanophase Sr, Mg, and Zn substituted hydroxyapatite by aqueous precipitation, *Mater. Sci. Eng. C* 35 (2014) 106–114

[34] Y. Sogo, T. Sakurai, K. Onuma, et al., The most appropriate (Ca<sub>2</sub>Zn)/P molar ratio to minimize the zinc content of ZnTCP/HAP ceramic used in the promotion of bone formation, *J. Biomed. Mater. Res.* 62 (2002) 457–463.

[35] A. Ito, K. Ojima, H. Naito, N. Ichinose, T. Tateishi, Preparation, solubility, and cytocompatibility of zinc-releasing calcium phosphate ceramics, *J. Biomed. Mater. Res.* 50 (2000) 178–183.

[36] E. Fujii, M. Ohkubo, K. Tsuru, S. Hayakawa, A. Osaka, K. Kawabata, C. Bonhomme, F. Babonneau, Selective protein adsorption property and characterization of nano-crystalline zinc-containing hydroxyapatite, *Acta Biomater.* 2 (2006) 69–74.

[37] Y. Tang, H.F. Chappell, M.T. Dove, R.J. Reeder, Y.J. Lee, Zinc incorporation into hydroxyapatite, *Biomaterials* 30 (2009) 2864–2872.

[38] A. Ito, H. Kawamura, M. Otsuka, M. Ikeuchi, H. Ohgushi, K. Ishikawa, K. Onuma, N. Kanzaki, Y. Sogo, N. Ichinose, Zinc-releasing calcium phosphate for stimulating bone formation, *Mater. Sci. Eng. C* 22 (2002) 21–25.

[39] F. Miyaji, Y. Kono, Y. Suyama, Formation and structure of zinc substituted calcium hydroxyapatite, *Mater. Res. Bull.* 40 (2005) 209–220.

[40] A. Bigi, E. Foresti, M. Gandolfi, M. Gazzano, N. Roveri, Inhibiting effect of zinc on hydroxyapatite crystallization, *J. Inorg. Biochem.* 58 (1995) 49–58.

[41] G. Suresh Kumar, A. Thamizhavel, Y. Yokogawa, et al., Synthesis, characterization and in vitro studies of zinc and carbonate co-substituted nano-hydroxyapatite for biomedical applications, *Mater. Chem. Phys.* 134 (2012) 1127–1135.

[42] V. Stanic, S. Dimitrijevic, J. Antic-Stankovic, M. Mitric, B. Jokic, I.B. Plecas, S. Raicevic, Synthesis, characterization and antimicrobial activity of copper and zinc-doped hydroxyapatite nanopowders, *Applied Surface Science*, Volume 256, Issue 20,1 August 2010, Pages 6083-6089, <https://doi.org/10.1016/j.apsusc.2010.03.124>

[43] S.J. Kalita, H.A. Bhatt, Nanocrystalline hydroxyapatite doped with magnesium and zinc: Synthesis and characterization, *Materials Science and Engineering: C* Volume 27, Issue 4, 16 May 2007, Pages 837-848

[44] Yajing Yan, Xuejiao Zhang, Yong Huang, Qiongqiong Ding, Xiaofeng Pang, Antibacterial and bioactivity of silver substituted hydroxyapatite/TiO<sub>2</sub> nanotube composite coatings on titanium, *Applied Surface Science* 314 (2014) 348–357

[45] Cong Fu, Xuefei Zhang, Keith Savino, Paul Gabrys, Yun Gao, Wanaruk Chaimayo, Benjamin L. Miller b, Matthew Z. Yates, Antimicrobial silver-hydroxyapatite composite coatings through two-stage electrochemical synthesis, *Surface & Coatings Technology* 301 (2016) 13–19

[46] Anish Shivaram, Susmita Bose, Amit Bandyopadhyay, Mechanical degradation of TiO<sub>2</sub> nanotubes with and without nano-particulate silver coating, *journal of the mechanical behavior of biomedical materials* 59 (2016) 508-518

[47] Xiong Lu, Bailin Zhang, Yingbo Wang, Xianli Zhou, Jie Weng, Shuxin Qu, Bo Feng, Fumio Watari, Yonghui Ding and Yang Leng, Nano-Ag-loaded hydroxyapatite coatings on titanium surfaces by electrochemical deposition *J. R. Soc. Interface* (2011) 8, 529–539

[48] Chao-Ming Xie, Xiong Lu, Ke-Feng Wang, Fan-Zhi Meng, Ou Jiang, Hong-Ping Zhang, Wei Zhi, and Li-Ming Fang, Silver Nanoparticles and Growth Factors Incorporated Hydroxyapatite Coatings on Metallic Implant Surfaces for Enhancement of Osteo-inductivity and Antibacterial Properties, *Applied materials & Interfaces*

[49] M. Furko, Y. Jiang, T.A. Wilkins, Balázs, Electrochemical and morphological investigation of silver and zinc modified calcium phosphate bio-ceramic coatings on metallic implant materials, *Materials Science and Engineering C* 62 (2016) 249–259

[50] Zhang, B. L., Wang, Y. B., Lu, X., Zhou, X. L., Qu, S. X., Feng, B. & Weng, J. In press. Accepted HA/Ag composite coatings prepared by pulse electrochemical deposition on titanium surfaces. *Rare Metal Mater. Eng.*

[51] Liu, R. F., Xiao, X. F., Zhen, L. Q. & Huang, J. M. HA/Ag composite coatings prepared by two-step electro-deposition. *Chin. J. Appl. Chem.* 2003, 20, 547–551.

[52] B.S. Necula, I. Apachitei, F.D. Tichelaar, L.E. Fratila-Apachitei, J. Duszczyk , An electron microscopical study on the growth of TiO<sub>2</sub>–Ag antibacterial coatings on Ti6Al7Nb biomedical alloy, *Acta Biomaterialia* 7 (2011) 2751–2757

[53] Gary A. Fielding, Mangal Roy, Amit Bandyopadhyay, Susmita Bose, Antibacterial and biological characteristics of silver containing and strontium doped plasma sprayed hydroxyapatite coatings, *Acta Bio-materialia* 8 (2012) 3144–3152

[54] Yikai Chen, Xuebin Zheng, Youtao Xie, Chuanxian Ding, Hongjiang Ruan, Cunyi Fan, Anti-bacterial and cytotoxic properties of plasma sprayed silver-containing HA coatings, *J Mater Sci: Mater Med* (2008) 19:3603–3609

[55] Jinhua Li, Xuanyong Liu, Yuqin Qiao, Hongqin Zhu, Chuanxian Ding, Antimicrobial activity and cytocompatibility of Ag plasma-modified hierarchical TiO<sub>2</sub> film on titanium surface, *Colloids and Surfaces B: Biointerfaces* 113 (2014) 134–145

[56] Venkateswarlu Kotharu, Rameshbabu Nagumothua, Chandra Bose Arumugam, Muthupandi Veerappan, Subramanian Sankaran, MubarakAli Davoodbasha, Thajuddin Nooruddin, Fabrication of corrosion resistant, bioactive and antibacterial silver substituted hydroxyapatite/titania composite coating on Cp Ti, *Ceramics International* 38 (2012) 731–740

[57] Mangal Roy, Gary A. Fielding, Haluk Beyenal, Amit Bandyopadhyay, and Susmita Bose, Mechanical, In vitro Antimicrobial, and Biological Properties of Plasma-Sprayed Silver-Doped Hydroxyapatite Coating, *Applied materials & Interfaces*

[58] Baoe Li, Xuanyong Liu, Fanhao Meng, Jiang Chang, Chuanxian Ding, Preparation and antibacterial properties of plasma sprayed nano-titania/silver coatings, *Materials Chemistry and Physics* 118 (2009) 99–104

[59] S. Ciucă, M. Badea, E. Pozna, I. Pana, A. Kiss, L. Floroian, A. Semenescu, C.M. Cotrut, M. Moga b, A. Vladescu, Evaluation of Ag containing hydroxyapatite coatings to the *Candida albicans* infection, *Journal of Microbiological Methods* 125 (2016) 12–18

[60] W. Chena, Y. Liua, H.S Courtney, M. Bettenga, C.M. Agrawal, J.D. Bumgardnere, J.L. Ong, In vitro anti-bacterial and biological properties of magnetron co-sputtered silver-containing hydroxyapatite coating, *Biomaterials* 27 (2006) 5512–5517

[61] M. Badea, M. Braic, A. Kiss, M. Moga, E. Pozna, I. Pana, A. Vladescu, Influence of Ag content on the antibacterial properties of SiC doped hydroxyapatite coatings, *Ceramics International* 42 (2016) 1801–1811

[62] A. Balamurugan G. Balossier , D. Laurent-Maquin , S. Pina , A.H.S. Rebelo, J. Faure , J.M.F. Ferreira, An in vitro biological and anti-bacterial study on a sol–gel derived silver-incorporated bioglass system, *dental materials* 24 (2008) 1343–1351

[63] W. Chen, S. Oh, A.P. Ong, N. Oh, Y. Liu,4 H.S. Courtney, M. Appleford, J.L. Ong, Antibacterial and osteogenic properties of silver-containing hydroxyapatite coatings produced using a sol gel process, *Wiley InterScience* ([www.interscience.wiley.com](http://www.interscience.wiley.com)). DOI: 10.1002/jbm.a.31197

[64] Swarna Jaiswal, Patrick McHale, Brendan Duffy, Preparation and rapid analysis of antibacterial silver, copper and zinc doped sol–gel surfaces, *Colloids and Surfaces B: Biointerfaces* 94 (2012) 170–176

[65] O. Akhavan, E. Ghaderi, Self-accumulated Ag nanoparticles on mesoporous TiO<sub>2</sub> thin film with high bactericidal activities, *Surface & Coatings Technology* 204 (2010) 3676–3683

[66] Zhen Geng, Zhenduo Cui, Zhaoyang Li, Shengli Zhu, Yanqin Liang, Yunde Liu, Xue Li, Xin He, Xiaoxu Yu, Renfeng Wang, Xianjin Yang, Strontium incorporation to optimize the antibacterial and biological characteristics of silver-substituted hydroxyapatite coating, *Materials Science and Engineering C* 58 (2016) 467–477

[67] Chao Shi, Jianyong Gao, Ming Wang, Jingke Fu, Dalin Wang, Yingchun Zhu, Ultra-trace silver-doped hydroxyapatite with non-cytotoxicity and effective antibacterial activity, *Materials Science and Engineering C* 55 (2015) 497–505

[68] Brajendra Singh, Ashutosh Kumar Dubey, Samayendra Kumar, Naresh Saha, Bikramjit Basu, Rajeev Gupta, In vitro biocompatibility and antimicrobial activity of wet chemically prepared

Ca<sub>10-x</sub>Ag<sub>x</sub>(PO<sub>4</sub>)<sub>6</sub>(OH)<sub>2</sub> (0.0≤x≤0.5) hydroxyapatites, Materials Science and Engineering C 31 (2011) 1320–1329

[69] Mustafa Turkoz, Aykan Onur Atilla, Zafer Evis, Silver and fluoride doped hydroxyapatites: Investigation by microstructure, mechanical and antibacterial properties, Ceramics International 39 (2013) 8925–8931

[70] Carmen Steluta Ciobanu, Florian Massuyeau, Liliana Violeta Constantin and Daniela Predoi, Structural and physical properties of antibacterial Ag-doped nano hydroxyapatite synthesized at 100°C, Ciobanu et al. Nanoscale Research Letters 2011, 6:613

[71] A. Yanovsk, V. Kuznetsov, A. Stanislavov, S. Danilchenko, L. Sukhodub, Calcium–phosphate coatings obtained biomimetically on magnesium substrates under low magnetic field, Applied Surface Science 258 (2012) 8577–8584

[72] Anchun Mo, Juan Liao, Wei Xu, Suqin Xian, Yubao Li, Shi Bai, Preparation and antibacterial effect of silver–hydroxyapatite/titania nanocomposite thin film on titanium, Applied Surface Science 255 (2008) 435–438

[73] Andrea Ewald, Daniel Hösel, Sarika Patel, Liam M. Grover, Jake E. Barralet, Uwe Gbureck, Silver-doped calcium phosphate cements with antimicrobial activity, Acta Biomaterialia 7 (2011) 4064–4070

[74] Xiao Bai, Stefan Sandukas, Mark Appleford, Joo L. Ong, Afsaneh Rabiei, Antibacterial effect and cytotoxicity of Ag-doped functionally graded hydroxyapatite coatings, Wiley Online Library (wileyonlinelibrary.com). DOI: 10.1002/jbm.b.31985

[75] B. Bracci, P. Torricelli, S. Panzavolta, E. Boanini, R. Giardino, A. Bigi, Effect of Mg<sup>2+</sup>, Sr<sup>2+</sup>, and Mn<sup>2+</sup> on the Chemico-Physical and In Vitro Biological Properties of Calcium Phosphate, Biomimetic Coatings, Journal of Inorganic Biochemistry, 103 (2009) 1666

[76] Y. Huang, Q. Ding, X. Pang, S. Han, Y. Yan, Corrosion behavior and biocompatibility of strontium and fluorine co-doped electrodeposited hydroxyapatite coatings, Applied Surface Science 282 (2013) 456–462

[77] Yong Huang, Xuejiao Zhang, Honglei Zhang, Haixia Qiao, Xiaoyun Zhang, Tianjun Jia, Shuguang Hanb, Yuan Gaod, Hongyuan Xiaoe, Hejie Yang, Fabrication of silver- and strontium-doped hydroxyapatite/TiO<sub>2</sub> nanotube bilayer coatings for enhancing bactericidal effect and osteo-inductivity, Ceramics International 43 (2017) 992–1007

[78] Yajing Yan, Xuejiao Zhang, Caixia Li, Yong Huang, Qiongqiong Ding, Xiaofeng Pang, Preparation and characterization of chitosan-silver/hydroxyapatite composite coatings on TiO<sub>2</sub> nanotube for biomedical applications, Applied Surface Science 332 (2015) 62–69

[79] Vraneanu, D. M., Tran, T., Ungureanu, E., Negoiescu, V., Tarcolea, M., Dinu, M., Vladescu A, Zamfir R., Timotin A.C., Cotrut, C. M. (2018). Pulsed electrochemical deposition of Ag doped hydroxyapatite bioactive coatings on Ti6Al4V for medical purposes. Univ. Politeh. Buchar. Sci. Bull. Ser. B Chem. Mater. Sci, 80, 173–184.

[80] Thi Thanh TRAN, Cosmin Mihai COTRUT, Maria Diana VRANCEANU, Elena UNGUREANU, Mihai TARCOLEA, Studies of micro-structure and composition of the modified HA<sub>p</sub> coating via SEM investigations, Scientific Bulletin U.P.B 2020, Series B - Chemistry and Materials Science

[81] A. Vladescu, D.M. Vraneanu, S. Kulesza, A. N. Ivanov, M. Bramowicz, A.S. Fedonnikov, M. Braic, I.A. Norkin, A. Koptyug, M. Kurtukova, M. Dinu, I. Pana, M.A. Surmeneva, R.A. Surmenev, Cosmin M. Cotruț, Influence of the electrolyte's pH on the properties of electrochemically deposited hydroxyapatite coating on additively manufactured Ti64 alloy, Scientific reports, 7(1) (2017), Article Number: 16819, DOI: 10.1038/s41598-017-16985-z;

[82] Tadashi Kokubo, Hiroaki Takadama, How useful is SBF in predicting in vivo bone bioactivity? Biomaterials 27 (2006) 2907–2915

[83] Vraneanu, D. M., Parau, A. C., Cotrut, C. M., Kiss, A. E., Constantin, L. R., Braic, V., & Vladescu, A. (2019). In vitro evaluation of Ag doped hydroxyapatite coatings in acellular media. Ceramics International, 45(8), 11050-11061